

Myosin-1C augments secretion of von Willebrand factor by linking contractile actomyosin machinery to the plasma membrane

Tracking no: ADV-2024-012590R2

Sammy El-Mansi (Queen Mary University of London, United Kingdom) Tom Mitchell (Queen Mary University of London, United Kingdom) Golzar Mobyen (Imperial College London, United Kingdom) Thomas McKinnon (Imperial College London, United Kingdom) Pika Miklavc (University of Salford, United Kingdom) Manfred Frick (Ulm University, Germany) Thomas Nightingale (Queen Mary University of London, United Kingdom)

Abstract:

Blood endothelial cells control the hemostatic and inflammatory response by secreting von Willebrand factor (VWF) and P-selectin from storage organelles called Weibel-Palade bodies (WPB). Actin-associated motor proteins regulate this secretory pathway at multiple points. Prior to fusion, myosin Va forms a complex that anchors WPBs to peripheral actin structures allowing maturation of content. Post-fusion, an actomyosin ring/coat is recruited and compresses the WPB to forcibly expel the largest VWF multimers. Here we provide the first evidence for the involvement of class I myosins during regulated VWF secretion. We show that the unconventional myosin-1C (Myo1c) is recruited post-fusion via its pleckstrin homology domain in an actin-independent process. This provides a link between the actin ring and phosphatidylinositol 4,5-bisphosphate (PIP2) at the membrane of the fused organelle and is necessary to ensure maximal VWF secretion. This is an active process requiring Myo1c ATPase activity as inhibition of class I myosins using the inhibitor Pentachloropseudilin or expression of an ATPase deficient Myo1c rigor mutant perturbs the expulsion of VWF and alters the kinetics of the exocytic actin ring. These data offer a novel insight into the control of an essential physiological process and provide a new way in which it can be regulated.

Conflict of interest: No COI declared

COI notes:

Preprint server: Yes; bioRxiv <https://doi.org/10.1101/2023.08.11.552954>

Author contributions and disclosures: S.E.-M., and T.D.N., developed the methodology; P.M. and M.F. generated and provided essential tools and reagents; S.E.-M., T.D.N., T.P.M., T.A.J.M and G.M performed the investigation; T.D.N. supervised the study; S.E.-M. and T.D.N. wrote the original draft; and all authors reviewed and edited the manuscript.

Non-author contributions and disclosures: No;

Agreement to Share Publication-Related Data and Data Sharing Statement: Mass Spectrometry data is available via the PRIDE40 partner repository with the dataset identifier PXD036983 and 10.6019/PXD036983. For other original data and constructs, please contact t.nightingale@qmul.ac.uk

Clinical trial registration information (if any):

TITLE

Myosin-1C augments endothelial secretion of von Willebrand factor by linking contractile actomyosin machinery to the plasma membrane

SHORT TITLE

Myosin-1C augments endothelial secretion of VWF

AUTHORS

Sammy El-Mansi^{1†}, Tom P. Mitchell¹, Golzar Mobayen², Thomas A. J. McKinnon², Pika Miklavc³, Manfred Frick⁴, Thomas D. Nightingale^{1†}

AFFILIATIONS

1. Centre for Microvascular Research, William Harvey Research Institute, Barts and the London School of Medicine and Dentistry, Queen Mary University of London, London EC1M 6BQ, UK.

2. Department of Immunology and Inflammation, Centre for Haematology, Imperial College London, Hammersmith Hospital Campus, London, United Kingdom

3. School of Science, Engineering & Environment, University of Salford, Manchester M5 4WT, UK.

4. Institute of General Physiology, Ulm University, Albert-Einstein-Allee 11, 89081 Ulm, Germany.

† Corresponding authors: s.elmansi@qmul.ac.uk and t.nightingale@qmul.ac.uk

Correspondence

Sammy El-Mansi and Thomas D. Nightingale, Centre for Microvascular Research, William Harvey Research Institute, Charterhouse Square, Faculty of Medicine and Dentistry, Queen Mary University of London, London EC1M 6BQ, United Kingdom; e-mail: s.elmansi@qmul.ac.uk and t.nightingale@qmul.ac.uk.

Mass Spectrometry data is available via the PRIDE40 partner repository with the dataset identifier PXD036983 and 10.6019/PXD036983. For other original data and constructs, please contact t.nightingale@qmul.ac.uk

WORD COUNT: 4087

ABSTRACT (200 words)

Blood endothelial cells control the hemostatic and inflammatory response by secreting von Willebrand factor (VWF) and P-selectin from storage organelles called Weibel-Palade bodies (WPB). Actin-associated motor proteins regulate this secretory pathway at multiple points. Prior to fusion, myosin Va forms a complex that anchors WPBs to peripheral actin structures allowing maturation of content. Post-fusion, an actomyosin ring/coat is recruited and compresses the WPB to forcibly expel the largest VWF multimers. Here we provide the first evidence for the involvement of class I myosins during regulated VWF secretion. We show that the unconventional myosin-1C (Myo1c) is recruited post-fusion via its pleckstrin homology domain in an actin-independent process. This provides a link between the actin ring and phosphatidylinositol 4,5-bisphosphate (PIP2) at the membrane of the fused organelle and is necessary to ensure maximal VWF secretion. This is an active process requiring Myo1c ATPase activity as inhibition of class I myosins using the inhibitor

Pentachloropseudilin or expression of an ATPase deficient Myo1c rigor mutant perturbs the expulsion of VWF and alters the kinetics of the exocytic actin ring. These data offer a novel insight into the control of an essential physiological process and provide a new way in which it can be regulated.

Key points

1. Myosin-1C is utilized for actomyosin mediated expulsion of an essential blood clotting factor (von Willebrand factor).
2. Myosin-1C links the exocytic actomyosin ring to PIP2 on the plasma membrane forming anchor points that allow maximal VWF secretion.

INTRODUCTION

Endothelial cells (EC) contain rod-shaped storage organelles called Weibel-Palade bodies (WPB)¹ which owe their unique shape to their main cargo: the pro-hemostatic glycoprotein, von Willebrand factor (VWF).² VWF dimerizes in the endoplasmic reticulum and concatemerizes as it passes through the trans Golgi network (TGN) forming long parallel proteinaceous tubules that are packaged into WPB. Other cargo include the pro-inflammatory receptor P-selectin,³ cytokines and agents that control tonicity; thus, exocytosis of WPB is a crucial event important during hemostasis and inflammation.⁴

Regulated secretion of VWF occurs rapidly in response to stimulation with secretagogues released during injury and inflammation.^{5,6} Secreted VWF tubules unfurl to form strings (up to 1 mm long) anchored to the EC surface. These serve as a platform for platelet aggregation and thrombus formation.⁷ This process instigates the primary hemostatic response but is also causally associated with thrombotic diseases such as peripheral vascular disease, myocardial infarction and stroke.⁸ Responsible for one in four deaths,⁹ thrombosis is a leading cause of death world-wide. While current therapy options are numerous, they are complicated by the risk of excess bleeding and cerebral hemorrhage.¹⁰ As such, there remains a profound medical need for more nuanced treatment strategies.

Circulating levels of VWF are prognostic for cardiovascular disease¹¹ and control of regulated secretion of VWF is being actively investigated as a therapeutic strategy to reduce the burden of thrombotic diseases. Aptamers and antibodies targeting VWF are currently being tested in the clinic to limit thrombotic pathologies such as thrombotic thrombocytopenic purpura¹² and stroke.¹³ We have previously identified cellular machinery that regulates the expulsion of VWF and targeting this process represents an exciting therapeutic approach. ECs recruit actin and non-muscle myosin to sites of WPB exocytosis as rings, these contract in a process aided by septins¹⁴ to forcibly extrude the ultra large VWF multimers apically (into the blood vessel lumen).¹⁵

Myosins are molecular motor proteins that mediate organelle trafficking and contractile processes during muscle contraction, cytokinesis and protein secretion.¹⁶⁻¹⁸ Conventional class II myosins dimerize and bind to adjacent, oppositely orientated, actin filaments via both head regions to exert force. This is known as the 'sliding filament hypothesis'.¹⁹ Monomeric class I myosins are referred to as unconventional and lack these abilities. They are localized at cell membranes in ruffles, filopodia and the leading edge during migration.¹⁷ Structurally, class I myosins are composed of an actin and ATP-binding head domain, a variable neck region and a tail domain.²⁰ The 'neck' (or lever) region contains calmodulin (light chain) binding IQ (isoleucine-glutamine) motif(s) which acts as a regulatory domain, similar to the light chains of class II myosins.²¹ Lastly, class I myosins possess a pleckstrin homology (PH) domain in the tail region that facilitates binding to phosphoinositides.²² In some settings, class I myosins transport intracellular vesicles along actin filaments.^{23,24} They have also been shown to tether GLUT4-containing vesicles to actin during exocytosis.²⁵ Whereas lung surfactant secreting alveolar type II (ATII) cells utilize actin and class I myosins to aid vesicle compression during lamellar body exocytosis.²⁶

A pivotal role of a subset of myosin isoforms in WPB trafficking and VWF secretion has previously been described. WPB are anchored to actin structures in the cell periphery by a tripartite complex of Rab27a, MyRIP and Myosin Va.^{27,28} Non-muscle myosin IIA (NMIIA),²⁹ NMIIB¹⁵ and Myosin Vc³⁰ have been implicated in the actomyosin mediated expulsion of VWF. However, the role of class I myosins has not been characterized.

We previously utilized peroxidase proteomics to identify proteins in close proximity to WPB in unstimulated and stimulated conditions.¹⁴ This powerful approach identified differential proximity of actin-binding motor proteins to the WPB surface in resting ECs and in response to stimuli. Here, we describe the function of the class I myosin motor, myosin 1C (Myo1c) and suggest a crucial role in linking the contractile actin ring to the plasma membrane (PM) to augment vesicle compression.

METHODS

Cell culture

Human Umbilical Vein ECs (HUVEC) (Cat: 12203) and Human Dermal Microvascular ECs (HDMEC) (Cat: 12212) were purchased from PromoCell. ECs were cultured as described elsewhere.³¹ HDMEC were cultured using PromoCell Ready-to-use Growth Medium MV (Cat: 22020).

Immunofluorescence and western blotting

This was performed exactly as described elsewhere.¹⁵ The commercial suppliers of antibodies used here are provided in Table S1. Confocal imaging was performed using the Zeiss LSM 800 and Nikon CSU-W1 SoRa spinning disk microscope with 0.1-0.2 μ m interval Z stacks for fixed sample imaging. Where necessary image brightness and contrast was adjusted for clarity and in alignment with the American Society of Hematology Author Guidelines.

Live cell imaging

Myo1c-GFP, Myo1c-Tail+3IQ-GFP, Myo1c-K892A-GFP and Myo1c-R903A-GFP were kind gifts from Michael Ostap.²² PH-PLC δ 1-GFP was a gift from Christian Halaszovich.³² GFP-Myo1c was a gift from Martin Bähler (Addgene plasmid # 134832).³³ GFP-Myo1c (G108R) was generated in our laboratory. GFP-PIPK1 gamma 87 was a gift from Pietro De Camilli (Addgene plasmid # 22300).³⁴ GFP-VWF was a gift from J. Voorberg and J.A. Van Mourik (Sanquin Research Laboratory, Amsterdam, Netherlands).³⁵ P-Selectin luminal domain mCherry (P.sel.lum.mCherry) was previously cloned in our laboratory.¹⁵ LifeAct-GFP was a gift from B. Baum (University College London, London, England, UK).³⁶ HUVEC were incubated at 37C, 5% CO₂ and 0.5-1 μ m interval Z stacks were obtained continuously for 5-10 minutes according to experimental objective.

Myo1C mutagenesis

Mutation of glycine 108 to arginine (G108R) changes a conserved residue of the nucleotide binding region in the motor domain and results in a rigor mutant.^{37 38} The rigor mutant was generated as described in Edelhei et al.,³⁹ using the forward primer 5' gatttctggagagagtcgggcaggcaagaca 3' and the reverse primer 5' gtcttgctgccccgactctctccagaatc 3'. Mutated residues are shown in bold, isolated clones were sequenced for verification.

Assessment of target protein inhibition on VWF secretion using NIR fluorescent dot blot

siRNAs targeting Myo1c (Cat: L-015121-00-0005) were purchased as SMARTpools from Dharmacon (Horizon Discovery). Firefly luciferase targeted siRNA was made by Eurofins Genomics (sequence 5' cgu-acg-cgg-aau-acu-ucg 3'). Electroporation of HUVEC, VWF secretion assay and near-infrared (NIR)-fluorescent dot blot was performed as described in our previous research.¹⁴ Phorbol 12-myristate 13-acetate (PMA) (100 ng/mL), thrombin (1 U/mL), vascular endothelial growth factor (VEGF) (40 ng/mL), histamine (100 μ M), adrenaline (10 μ M) or 3-isobutyl-1-methyl xanthine (IBMX) (100 μ M) were used to stimulate WPB exocytosis. For myosin 1 inhibition, HUVEC were exposed to Pentachloropseudilin (PCLP) (AOBIOUS, Cat: AOB33969) for 30 mins or 16 hours (5-20 μ M) prior to stimulation with secretagogue.

In vivo

Procedures conducted using mice were in alignment with the institutional Animal Welfare Ethical Review Body (AWERB) and UK Home Office guidelines. Eight-week-old, male, C57BL/6 mice (Charles River, UK) were housed under controlled environmental conditions (12-hour light/dark cycles at ambient temperature and humidity) on a standard chow diet. Whole-mount staining and imaging of cremasteric venules was performed as described elsewhere.⁴⁰

RESULTS

APEX2 proximity proteomics identified differentially enriched myosin isoforms as putative regulators of WPB dynamics

Myosin isoforms have pleiotropic functions in secretory vesicle trafficking. They are essential for pre- and post-fusion exocytic processes, including the anchoring of vesicles to peripheral actin, remodelling of cortical actin, stabilization/linking the fusion pore to the PM and force-driven compression to mediate cargo expulsion.⁴² In order to discern which myosin isoforms were of importance in regulated VWF secretion we consulted our publicly available proximity proteomics data set.¹⁴

A volcano plot was generated to illustrate which myosin isoforms were most upregulated and most significantly enriched proximal to WPBs (Fig. 1A). Myosin Va (MYO5A), forms a tripartite complex with Rab27a and MYRIP in order to anchor WPBs to actin structures in the cell periphery.⁴³ As expected, Myosin Va was significantly enriched in both unstimulated and stimulated (PMA or Histamine/Adrenaline/IBMX [HAI]) Rab27a-proximity proteomic data sets.¹⁴ Unexpectedly, the class IX myosin, Myosin 9B (Myo9B) was the most highly enriched and statistically significant myosin isoform proximal to WPBs in both resting and stimulated cells. This was confirmed using immunofluorescence (IF), where some Myo9B (green) could be seen proximal VWF (blue) near actin structures (magenta) and likely at focal adhesions (Fig. 1B). This unusual myosin motor has a Rho-GAP domain in its tail region.⁴⁴ As Rho activation has previously been implicated in VWF secretion^{45,46} we did not anticipate that Myo9B was a positive regulator of VWF secretion. Indeed, knockdown (~82%) of Myo9B by siRNA did not affect VWF secretion following exposure to distinct secretagogues (Fig. 1C&D). Subsequently, we chose to investigate the class I myosin family, of which two isoforms were significantly enriched in proximity to WPBs (isoforms C and E) (Fig. 1A: Bold). Of these, only Myo1c was enriched exclusively following secretagogue stimulation (both PMA and HAI), indicating a potential role in regulated exocytosis. To assess the functional role of Myo1c we assessed the effect of depleting the endogenous pool of Myo1c on regulated VWF secretion. SiRNA mediated depletion resulted in knock down efficiencies of 71-88% (Fig. 1E). In agreement with a role in WPB exocytosis, Myo1c knock down reduced VWF secretion in response to PMA ($p < 0.005$) (Fig. 1F). Through use of independent siRNAs against Myo1c (Fig. S1A-C) we confirmed depletion of Myo1c reduced VWF secretion in response to PMA and HAI. Furthermore, Myo1c KD reduced VWF secretion in response to the potent physiological regulators of VWF secretion VEGF165 ($p < 0.05$) (Fig. 1G) and thrombin ($p < 0.01$) (Fig. S1D). A complicating factor is that Myo1c depletion has been reported to disrupt recycling of lipid rafts⁴⁷ and the trafficking of VEGFR2 to the PM resulting in lysosomal degradation.⁴⁸ We confirmed that endogenous VEGFR2 concentrations were significantly reduced in Myo1c KD cells ($p < 0.01$) (Fig. 1H&I) as well as in HUVEC treated overnight with the pan class I myosin inhibitor, PCLP ($p < 0.5$) (Fig. 1J&K). To avoid this as a confounding factor in our investigations, we hereafter used PMA as the experimental secretagogue as this chemical is a cell permeable PKC activator bypassing PM-receptor signalling.

Myo1c is recruited during exocytosis

Myo1c has proposed roles in membrane fusion of GLUT4 containing vesicles,⁴⁹ compression of lung surfactant secreting lamellar bodies²⁶ and for linking actin to the PM during compensatory endocytosis in frog eggs.⁵⁰ IF and super-resolution spinning disk microscopy of HUVEC showed that Myo1c did not co-localize with VWF in unstimulated cells (Fig. 2A: box and inset). Following secretagogue stimulation WPBs fuse with the PM and collapse as the pH of the organelle shifts from acidic to neutral⁴ and Myo1c was apparent surrounding fused WPB. Endogenous Myo1c was localized as punctae within the actin ring but encapsulating VWF (Fig. 2A and Fig. S2A&B). Utilising the actin polymerization inhibitor, cytochalasin E (CCE) with and without stimulus, we noted that Myo1c recruitment is independent of actin (Fig. 2A). As a complementary approach, we utilized live cell imaging of HUVEC transiently expressing GFP-tagged Myo1c.³³ Co-expression with LifeAct-Ruby illustrated its colocalization with actin at the leading edge⁵¹ (Movie S1). Whereas co-expression with P.sel.lum.mCherry¹⁵ (a fusion marker which is stored in WPBs and lost upon fusion with the PM) allowed assessment of Myo1c recruitment dynamics during WPB exocytosis. In response to PMA, Myo1c-GFP was clearly recruited to WPBs post-fusion and was present on $68.65\% \pm 6.17$ of events (Fig. 2B) (Movie S2). In agreement with this, addition of an Alexa Fluor conjugated anti-VWF antibody to the culture media during stimulation revealed that the Myo1c ring appeared before expulsion and labelling of VWF (Fig. S2C). By imaging HUVEC expressing LifeActRuby and Myo1c-GFP we noted that the Myo1c signal preceded recruitment of the actin ring (Fig. S2D).

To confirm our results in an alternative EC type we assessed whether human dermal microvascular ECs (HDMEC) utilized actin rings during WPB exocytosis. Live cell imaging of HDMEC expressing LifeAct-GFP and P.sel.lum.mCherry confirmed that this phenomenon is not specific to venous ECs from the umbilical vein (Fig. 2C). IF studies demonstrated that HDMEC also recruit Myo1c during VWF secretion (Fig. 2D). Once more, this was shown to be independent of actin. Through whole-mount IF imaging of the murine cremaster muscle we determined that microvascular ECs express Myo1c in vivo (Fig. S3). This demonstrates that HUVEC are a physiologically relevant model for studying Myo1c function and that Myo1c has a post-fusion role. For the remainder of the investigations, we used HUVEC as our model system.

PIP2 mediated recruitment of Myo1c

Phosphoinositides control targeted membrane traffic and are differentially distributed between cellular compartments.⁵² Myo1c has a PIP2 binding PH domain in its tail region.²² Based on research in ATII cells²⁶ we anticipated that Myo1c was potentially recruited to fusing WPBs via this region (Fig. 3A). Lipids on the organelle and PM play a variety of roles in exocytosis in diverse secretory systems.⁵³ Phosphatidic acid and PIP2 are likely important in WPB exocytosis as phospholipase D1 (PLD1) has an established role in VWF secretion.⁵⁴ PIP2 sensors (PH-PLC δ 1-YFP) and enzymes (PIP5K γ 87) have previously been shown to be recruited to site of WPB fusion.⁵⁵ We independently confirmed that GFP-PIP5K1 γ 87 (Fig. 3B) and PH-PLC δ 1-GFP (Fig. 3C) were present at sites of WPB fusion following collapse of the organelle. Interestingly, we on occasion noted the presence of GFP-positive vacuoles in GFP-PIP5K1 γ 87-expressing cells that were coated in Myo1c, actin and septin 7 (another lipid binding protein associated with WPB exocytosis) (Fig. S4). These data indicate the presence of PIP2 on the PM drives protein recruitment.

To investigate the mechanism of its recruitment we used truncated and point mutants of Myo1c (Fig. 3D). By co-expressing the GFP-tagged neck and tail domain of Myo1c (Myo1c-Tail+3IQ-GFP) together with LifeAct-Ruby we demonstrate that the N-terminus is necessary for appropriate Myo1c targeting to actin at the leading edge (Fig. 3E and inset) (Movie S3). Consistent with the hypothesis that Myo1c is recruited to fusing WPB via its tail-resident PH domain; Myo1c-Tail+3IQ-GFP localized to fused WPBs following secretagogue stimulation (Fig. 3F). We used a GFP-tagged Myo1c fusion proteins harbouring point mutations in the phosphoinositide-binding PH domain (K892A/R903A) to show that the interaction with PIP2 is necessary for recruitment to WPB at fusion (Fig. 3G&H). Unlike the wild type (WT) and Myo1c-Tail+3IQ construct; Myo1c-K892A-GFP and Myo1c-R903A-GFP localized to the cytosol and were not recruited to WPBs post-fusion. Taken together, these data indicate that Myo1c is recruited to WPB post-fusion via its PH domain.

The effect of type I myosin inhibition on VWF secretion and exocytic actin ring dynamics

To investigate the role of the motor (head) domain we utilized the pan-myosin I inhibitor, PCLP.⁵⁶ PCLP is a potent allosteric inhibitor of myosin ATPase which shows selectivity for class I myosins at low doses (IC₅₀ ~ 1-10 μ M). However, at higher doses, other myosin classes (e.g., NMIIIB IC₅₀ ~ 90 μ M)⁵⁶ are affected. Here, pre-exposure to 2.5-20 μ M PCLP for 16 hours resulted in an obvious trafficking defect whereby the endogenous levels of total and mature-VWF were decreased (Fig. 4A-C) ($p < 0.05$). The ratio of pro-VWF to mature-VWF was increased in a dose-dependent fashion (Fig. 4D) ($p < 0.05-0.01$). Regulated VWF secretion (Fig. 4E & F) and string formation (Fig. 4G-I) were almost completely abolished in PCLP treated cells. Moreover, IF of LAMP1 (Fig. 4J) and TGN46 (Fig. 4K) illustrated the appearance of VWF positive lysosomes and a gross defect in morphology of the TGN. This demonstrates that class I myosins play a role in VWF trafficking as well as secretion. To determine the specific role of Myo1c in VWF trafficking we next assessed the effect of four different siRNA oligonucleotides targeting Myo1c on VWF levels by western blotting. Quantification of the levels of mature and pro-VWF were unchanged by Myo1c knockdown indicating that Myo1c is not essential for WPB biogenesis. The broader effect of PCLP likely reflect effects on other class I myosins during WPB biogenesis (Fig. S5).

Short term PCLP treatment (30 minutes) allows post-fusion analysis of the role of type I myosins in WPB exocytosis by acutely inhibiting the myosin I ATPase activity without affecting WPB biogenesis (Fig. 5A). Accordingly, we first utilized PCLP to assess the effect on PMA-induced VWF secretion. Pre-incubation with 10-40 μ M PCLP significantly reduced VWF secretion ($p < 0.05-0.01$) (Fig. 5B). We next imaged HUVEC co-expressing GFP-VWF and P.sel.lum.mCherry to investigate the effect of type I myosin inhibition on VWF expulsion (Fig. 5C). PCLP significantly ($p < 0.01$) increased the lag time for GFP-VWF to be expelled following the loss of the WPB fusion marker, P.sel.lum.mCherry (61s \pm 9 vs 172s \pm 13 mean \pm SEM) (Fig. 5D&E). To address whether this result was specific to Myo1c or a broader effect on class I myosins we repeated this loss of function assay using siRNA. We achieved KD efficiencies of ~68% (Fig. 5F). This correlated with a marked increase in the average delay between the loss of P.sel.lum.mCherry and GFP-VWF (42s \pm 8.4 vs 99s \pm 10.2) (Fig. 5G). Given the heterogenous nature of siRNA transfection efficiencies across a monolayer of cells we postulate the phenotype is likely an underestimation and this indicates Myo1c is the predominant class I myosin influencing WPB exocytosis.

Next, we studied actin dynamics during WPB exocytosis using a similar approach substituting GFP-VWF for LifeAct-GFP (Fig. 6A). This demonstrated that type I myosin inhibition with PCLP had no effect on the percentage of WPB fusion events that recruited an actin ring (Fig. 6B). This indicated that Myo1c is not required for actin polymerization. However, an increased proportion of persisting (>60s) actin coats/rings was noted in PCLP treated cells (2.4% vs 19.3%) (Fig. 6C) demonstrating that actin ring contraction required Myo1c ATP hydrolysis (Movie S4&5). This phenotype was confirmed by generating a dominant negative GFP-Myo1c rigor mutant via the introduction of a point mutation in the ATP-binding site (G108R) (Fig. 6D). Live cell imaging of GFP-Myo1c WT and GFP-Myo1c (G108R) determined that both were recruited to WPBs during exocytosis and the percentage of fusion events that were positive for Myo1c-GFP signal was comparable to that of actin rings (WT 68.7% \pm 6.2 vs G108R 84.79% \pm 6.1) (Fig. 6E). The WT signal persisted for

approximately 26 secs which also matches the dynamics of the actin ring.^{14,15} However, the rigor mutant persisted for longer ($\sim 57s \pm 19$), mirroring what we observed when imaging actin dynamics in the presence of PCLP (Fig. 6F). This was also reflected in the distribution of frequency of events. We noted a striking similarity to the change in actin ring dynamics where the percentage GFP-Myo1c rings that lasted over 60s was increased following PCLP treatment (3.8% vs 11.9%) (Fig. 6G). Using an Alexa Fluor-conjugated anti-VWF antibody in the medium we monitored VWF as it is secreted from the cell (Fig. 6H). We compared the amount of VWF secreted by the cell in relation to total VWF whilst overexpressing GFP, GFP-Myo1c WT or GFP-Myo1c (G108R). Concordant with our previous data overexpression of the “rigor” mutant resulted in reduced secretion of VWF (Fig. 6I). However, this must be caveated with potential off target effects during WPB biogenesis at the TGN (Fig. 6H arrows and Fig. S6). Taken together these data indicate a role for Myo1c and its ATPase domain in augmenting compression of the vesicle likely through actin coat organization and linkage.

DISCUSSION

We previously described the presence of a contractile actomyosin ring that is recruited to the WPB surface following fusion with the PM and aiding efficient VWF secretion.¹⁵ This represents an unexploited therapeutic target for the prevention of thrombotic pathologies. Actomyosin mediated expulsion of VWF requires upstream protein kinase C α (PKC α)⁵⁷ and p21 activated kinase 2 (PAK2)¹⁴ signalling, Spire1 mediated actin nucleation,⁵⁸ zyxin and α -actinin mediated organization⁵⁹ and controlled compression (via septin¹⁴ and non-muscle myosin isoforms^{15,29}). However, the mechanism by which the actomyosin ring is attached to the vesicle membrane and how this influences exocytosis is unclear. We demonstrate that Myo1c is recruited to the membrane of fused WPBs by its PH domain, in an actin-independent fashion. Perturbation of Myo1c function through pharmacological inhibition or siRNA mediated depletion reduced VWF secretion in human ECs and detailed live cell imaging experiments implicate a role in augmenting WPB exocytosis through providing additional traction points for the actin ring. This represents the first description of how class I myosin motors contribute to endothelial secretion of VWF secretion.

As a functional read out, we assessed the effect of siRNA mediated depletion of Myo1c on VWF secretion in response to PMA and VEGF165. These secretagogues were chosen as they stimulate increases in cytosolic cAMP and activation of PKC which is thought to be required for ring recruitment.^{29,57,59} SiRNA depletion of Myo1c modestly reduced VWF secretion in response to PMA but a greater effect was observed when HUVEC were stimulated with VEGF165. Myo1c is known to regulate VEGFR2 trafficking to the PM and Myo1c KD leads to VEGFR2 degradation.⁴⁸ It is plausible that this is not specific to VEGFR2, but also other membrane bound receptors (notably we also saw a marked effect of Myo1c depletion on thrombin stimulated VWF release). For this reason, we draw our conclusions from investigations on ECs stimulated with the membrane permeable PKC agonist PMA.

Although other class I myosins such as Myo1e⁶⁰ have roles in other secretory systems, we have focused on delineating a role for Myo1c. In addition to actin-membrane tethering, Myo1c aids insulin stimulated PM-fusion of GLUT4 containing vesicles, where it is recruited prior to vesicle fusion.^{23,61} In contrast, we observed that GFP-tagged Myo1c is recruited to the WPB surface post-fusion, similar to that reported by Kittelberger and colleagues.²⁶ We therefore exclude that Myo1c is acting as an organelle transporter. Instead, we propose a similar role to that seen in surfactant exocytosis by ATII cells²⁶ and cortical granules in *Xenopus* eggs⁵⁰ whereby Myo1c links the actin coat to the vesicle membrane. To fulfil this role, Myo1c requires a tight interaction with both actin and the WPB membrane surface. We show that the PH domain of Myo1c binds PIP2 that is recruited to WPB post-fusion⁵⁵. Inhibition of the myosin head ATPase domain using PCLP resulted in constrained release of VWF and delayed actin ring contractility although it did not reduce the proportion of fusion events that recruited actin. We sought to confirm these findings by generating an ATP hydrolysis deficient (rigor) mutant (G108R). In the yeast homologue (Myo5), this mutation inhibits endocytosis and prevents membrane invagination.³⁸ A similar rigor mutant has also been generated by mutating a lysine 111 (K111R) that inhibits lipid raft exocytosis.⁴⁷ The Myo1c rigor mutant reduced the amount of VWF secreted and live cell imaging showed that it persisted at the site of fusion longer than the full-length Myo1c control. The timing of WT Myo1c recruitment mirrored the spatiotemporal dynamics of the actin ring further suggesting a role in aiding this force driven process. The change in ring kinetics following inhibition

with PCLP were strikingly similar to those of G108R. Overall, these changes closely resemble the defect in actin ring contraction observed when NMII isoforms are inhibited using blebbistatin¹⁵ consistent with active Myo1c augmenting VWF release by providing anchor points for the actomyosin ring.

Here, an acute PCLP exposure time of 30 minutes was needed to assess actin ring dynamics during WPB exocytosis. Longer incubation times had drastic effects on protein trafficking. Sixteen-hour incubation with PCLP resulted in disruption of the TGN, a near complete abrogation of regulated VWF secretion, ineffective VWF biogenesis as well as the clear observation of VWF signal in LAMP1 positive lysosomes. This may reflect defects at the Golgi⁶² or inhibition of autophagosome-lysosome fusion⁶³ with subsequent effects on WPB turnover, lysosomal co-localization and degradation of VWF. Importantly, we did not observe this phenotype in Myo1c depleted cells and therefore hypothesize that this trafficking defect is caused by inhibitory action of PCLP on other class I myosins.⁵⁶ Notably, Myo1b promotes the formation of tubules and carriers at remodelling TGN membranes⁶⁴ and has a role in secretory granule biogenesis in pancreatic Beta cells⁶⁵ and neuroendocrine cells.⁶⁶ A specific role in WPB biogenesis is therefore also a possibility.

Finally, as a hypothesis of the spatiotemporal recruitment of these molecules we present a putative working model (Graphical Abstract). Enriched PIP2 concentrations occur at the site of WPB fusion either as a result of membrane mixing and/or through PIPK1 γ 87 mediated production from its precursor PI4P. PIP2 at the WPB surface then leads to the rapid recruitment of Myo1c via its lipid binding PH domain. *De novo* Spire1 mediated actin nucleation⁵⁸ follows (or occurs simultaneously) with the Myo1c motor domain binding to the resulting actin coat/ring. We suggest that NMII isoforms are recruited after actin, such as seen in *Xenopus* eggs⁶⁷, lamellar bodies,⁶⁸ rodent⁶⁹ and *Drosophila* salivary granules.⁷⁰ Activation of these isoforms then leads to vesicle compression and expulsion of VWF.

Overall, these data provide the first evidence of class I myosins participating in VWF secretion from ECs. And to our knowledge this is the first description of a role for Myo1c in the field of thrombosis and hemostasis. As such these data aid our fundamental understanding of the molecular mechanisms governing primary hemostasis.

ACKNOWLEDGMENTS

The authors thank their funders and collaborators. This work was supported by the British Heart Foundation (Grant PG/22/11208). T.P.M. was funded by a Barts Charity Project Grant (MGU05434).

We acknowledge the CMR Advanced Bio-Imaging Facility of QMUL for the help and advice with microscopy. We thank Dr. Chris Stefan (University College London) for his critical appraisal of this manuscript.

AUTHORSHIP CONTRIBUTIONS

S.E.-M., and T.D.N., developed the methodology; P.M. and M.F. generated and provided essential tools and reagents; S.E.-M., T.D.N., T.P.M., T.A.J.M and G.M performed the investigation; T.D.N. supervised the study; S.E.-M. and T.D.N. wrote the original draft; and all authors reviewed and edited the manuscript.

DISCLOSURE OF CONFLICTS OF INTEREST

404 The authors declare no competing financial interests.

405 **CORRESPONDANCE**

406 Sammy El-Mansi and Thomas D. Nightingale, Centre for Microvascular Research, William
407 Harvey Research Institute, Charterhouse Square, Faculty of Medicine and Dentistry, Queen
408 Mary University of London, London EC1M 6BQ, United Kingdom; e-mail:
409 s.elmansi@qmul.ac.uk and t.nightingale@qmul.ac.uk.

FIGURE LEGENDS

Figure 1: WPB proximal myosin motors (A) Volcano plot of myosin isoforms in close proximity to WPBs, previously identified by Rab27a-targeted APEX2 proximity proteomics. Blue - significantly enriched in unstimulated cells. Green – significantly enriched in PMA stimulated cells. Magenta – significantly enriched in HAI stimulated cells. Grey - not statistically significant as compared to mock transfected HUVEC. Paired *t* test. (B) Unstimulated HUVEC were fixed and subject to immunofluorescence analysis to localize Myo9B (green) in relation to VWF (blue) and actin (magenta). Myo9B staining was present in the cytoplasm and at the end of actin stress fibres reminiscent of focal adhesions. In some cases, VWF localized proximal to Myo9B puncta. Scale bar 10 μ m. Inset 1 μ m (C) Western blotting of tubulin and Myo9b in HUVEC lysate following two rounds of electroporation of 300 pMoles luciferase (LUC) and Myo9B targeting siRNA. Representative blot. KD= knock down efficiency (D) VWF secretion in response to PMA, HAI and thrombin was assessed by NIR dot blot n=3. (E) Western blotting of tubulin and Myo1c in HUVEC lysate following two rounds of electroporation of 500 pM luciferase (LUC) and Myo1c targeting siRNA. (F) LUC and Myo1c KD HUVEC were exposed to PMA (100 ng/mL) or (G) VEGF165 (40 ng/mL) and VWF secretion was quantified by NIR dot blot. n=3. Students *t* test. ***P<0.005 **P<0.01. (H) Western blotting and (I) densitometry of Myo1c, VEGFR2 and GAPDH in LUC and Myo1c KD HUVEC (n=6). (J&K) HUVEC were treated with the pan class I myosin inhibitor PCLP for 16 hours and endogenous levels of GAPDH and VEGFR2 determined by western blotting. Oneway ANOVA *P<0.05 n=3.

Figure 2: Endothelial cells utilize Myo1c as part of the WPB exocytic machinery (A) Super resolution imaging and immunofluorescent localization of endogenous Myo1c (green), actin (magenta) and VWF (blue) in unstimulated or PMA (100 ng/ml) stimulated HUVEC in the presence and absence of 1 μ M of the actin polymerization inhibitor cytochalasin E (CCE). Scale bar 10 μ m. Inset 1 μ m. Myo1c is recruited independently of actin but was dependent on stimulation with PMA. (B) Myo1c-GFP encapsulates WPB post-fusion as determined by live cell super resolution spinning disk imaging of PMA stimulated (100 ng/mL) HUVEC co-expressing a Myo1c-GFP and the WPB fusion marker P.sel.lum.mCherry. Scale bar 1 μ m. Arrow indicates point of collapse/fusion of vesicle (C) Live cell imaging of LifeAct-GFP and P.sel.lum.mCherry expressing HDMEC indicated the utility of actin rings to expel VWF following stimulation. Scale bar 10 μ m. Inset 1 μ m. 0.5 μ m Z stacks were acquired continuously for 10 minutes (Zeiss LSM 800) (D) Confocal imaging and IF analyses of endogenous Myo1c in HDMEC that were left untreated or stimulated with PMA, CCE or CCE and PMA. White arrows illustrate where Myo1c is recruited to fused/collapsed WPB. Scale bar 10 μ m.

Figure 3: The PH domain of Myo1c is required for its recruitment during WPB exocytosis. (A) A schematic of the proposed spatiotemporal dynamics of Myo1c recruitment during WPB exocytosis. (B) Live cell imaging of the GFP-PIPK1 γ 87 and P.sel.lum.mCherry in secretagogue (HAI) stimulated HUVEC illustrates post-fusion recruitment. Two exocytic events are seen here. Scale bars are 1 μ m. White and magenta arrows indicate independent fusion events. (C) The PIP2 sensor PH-PLC δ 1-GFP is also recruited post fusion. Scale bars are 1 μ m (D) A schematic of the Myo1c structural domains and location of truncation or site directed mutations. (E) HUVEC co-expressing LifeAct-Ruby and Myo1c-Tail+3IQ-GFP indicated the importance of the myosin head domain for interacting with actin. Scale bars are

10 μ m (F) Myo1c-Tail+3IQ-GFP is recruited to WPBs post-fusion (G&H) GFP-tagged Myo1c fusion proteins harbouring mutations in their PH domain (K892A/R903A) are not recruited to WPBs during exocytosis. F, G & H Scale bars are 10 μ m. Inset scale bars are 1 μ m. For live cell confocal imaging experiments 0.5 μ m Z stacks were acquired continuously for 5-10 minutes (Zeiss LSM 800).

Figure 4: HUVEC exposed to PCLP for 16 hours exhibit a VWF trafficking defect.

HUVEC were exposed to DMSO or a range of concentrations of PCLP and incubated overnight (16 hours). (A) Immunoblotting of the resulting lysates displayed changes in pro- and mature-VWF in relation to tubulin. Densitometry indicated a decrease in (B) total VWF and (C) mature-VWF levels alongside a dose-dependent increase in the (D) ratio of pro/mature VWF. $n=4$ Ratio paired t test. $*P<0.05$ $**P<0.01$ $***P<0.005$ (E) 16-hour incubation with PCLP resulted in inhibition of regulated secretion of VWF in response to thrombin and (F) HAI. (G) HUVEC pre-incubated with DMSO or PCLP for 16 hours were stimulated with HAI for 10 minutes before application of 5 dyne/cm² shear stress. VWF strings were visualized by immunofluorescence and confocal microscopy. (H) The number and (I) length of VWF strings secreted under flow in response to HAI in the presence or absence of DMSO or PCLP ($n=3$). (J) IF analyses using anti-LAMP1 (green) and anti-VWF (blue) antibodies indicated numerous VWF positive lysosomes in PCLP treated cells. (K) IF analyses using anti-TGN46 (yellow) and anti-VWF (blue) antibodies indicated a gross defect in TGN morphology (fragmented and swollen) in PCLP treated cells. Scale bars 10 μ m. Inset scale bars 1 μ m.

Figure 5: Acute inhibition of class I myosins and Myo1c depletion perturbs the expulsion of VWF

(A) Schematic of Myo1c domains and mechanism of inhibition by PCLP. (B) Pharmacological inhibition of the ATP binding domain with 10-40 μ M PCLP reduces VWF release. ($n=6$) $*P<0.05$, $**P<0.01$ ratio paired t test. (C) Schematic of live cell imaging approach to study WPB fusion dynamics and VWF expulsion. Scale bar 1 μ m. (D) HUVEC were electroporated with the P.sel.lum.mCherry and GFP-VWF constructs and imaged by confocal microscopy. Preincubation with 20 μ M PCLP increased the time taken for VWF to be expelled following loss of the fusion marker (P.sel.lum.mCherry). Students t test $**P<0.01$. [$n=3$ DMSO: 9 cells, 63 events PCLP: 9 cells, 38 events Mean \pm SEM]. (E) A frequency distribution of events. (F) LUC and Myo1c KD HUVEC were used to test whether these effects were specific to Myo1c or a broader effect of class I myosins. Western blotting determined the efficiency of target protein knockdown. (G) Myo1c siRNA depletion increased the time taken for VWF to be expelled following loss of P.sel.lum.mCherry. Students t test $*P<0.05$.

Figure 6: Inhibition of Myo1 ATPase activity through pharmacological inhibition or point mutation (G108R) effects the actomyosin machinery associated with exocytosis.

(A) Schematic of live cell imaging approach to study actin dynamics during WPB exocytosis. Scale bar 1 μ m. (B) PMA stimulated HUVEC co-expressing LifeAct-GFP and P.sel.lum.mCherry in the presence or absence of PCLP. The percentage of WPB fusion events that recruited an actin ring were unchanged in DMSO and PCLP (20 μ M) treated cells. (C) The lifetime (secs) of LifeAct-GFP signal at fusion sites was quantified in DMSO and PCLP treated HUVEC. The distribution of frequency of events is presented here [$n=5$ DMSO: 15 cells, 81 events PCLP: 18 cells, 93 events Mean \pm SEM] (D) Schematic of site-directed mutagenesis for the generation of a Myo1c rigor mutant. (E) HUVEC co-expressing

GFP tagged Myo1c constructs and P.sel.lum.mCherry were stimulated with PMA and the percentage of exocytic events that recruit GFP-Myo1c WT or G108R was quantified (n=3 WT: 8 cells, 119 events G108R: 8 cells, 58 events) (F) HUVEC co-expressing GFP tagged Myo1c constructs and P.sel.lum.mCherry were stimulated with PMA and the duration of GFP signal in a ring shape forming at the site of WPB fusion was quantified. (n=3 WT: 9 cells, 79 events PCLP 9 cells, 42 events). (G) The distribution of frequency closely resembles actin ring dynamics - panel C. For live cell confocal imaging experiments 0.5 μ m Z stacks were acquired continuously for 5-10 minutes (Zeiss LSM 800). (H) HUVEC expressing GFP, GFP-Myo1c (WT) or (G108R) were stimulated with PMA (100 ng/ml) for 10 min and labelled for external VWF (red) and total VWF (blue). Scale bar 1 μ m. (I) Quantification of the ratio of externalized VWF to total VWF. *P<0.05 One way ANOVA. N=3 NTC= non-transfected control. Arrows indicate swollen intracellular VWF signal in cells expressing the G108R point mutant.

Graphical abstract: A working model for actomyosin mediated expulsion of VWF.

Under resting conditions WPB are anchored to peripheral actin structure via Rab27a/MyRIP/MyoVa. (1) Following stimulation WPB are trafficked to the plasma membrane where they will fuse. (2) An enrichment of PIP2 is present at the site of fusion, possibly also on the WPB surface. This could be through membrane mixing or through the catalytic activity of PIPK1 γ 87. (3) Myo1c is recruited to the WPB via its PIP2 binding PH domain. (4) Spire1 mediated *de novo* actin nucleation could either occur after Myo1c recruitment or simultaneously. (5) Recruitment of NMII isoforms likely happens after actin polymerization. Activation of NMII allows for the expulsion of VWF into the blood vessel lumen.

REFERENCES

1. Weibel ER, Palade GE. New cytoplasmic components in arterial endothelia *J Cell Biol.* 1964;23:101-112.
2. Wagner DD, Olmsted JB, Marder VJ. Immunolocalization of von Willebrand protein in Weibel-Palade bodies of human endothelial cells. *J Cell Biol.* 1982;95(1):355-360.
3. Larsen E, Celi A, Gilbert GE, et al. PADGEM protein: a receptor that mediates the interaction of activated platelets with neutrophils and monocytes. *Cell.* 1989;59(2):305-312.
4. McCormack JJ, Lopes da Silva M, Ferraro F, Patella F, Cutler DF. Weibel-Palade bodies at a glance. *Journal of Cell Science.* 2017;130(21):3611-3617.
5. Tsai HM, Nagel RL, Hatcher VB, Seaton AC, Sussman, II. The high molecular weight form of endothelial cell von Willebrand factor is released by the regulated pathway. *Br J Haematol.* 1991;79(2):239-245.
6. Sporn LA, Marder VJ, Wagner DD. Inducible secretion of large, biologically potent von Willebrand factor multimers. *Cell.* 1986;46(2):185-190.
7. Dong JF, Moake JL, Nolasco L, et al. ADAMTS-13 rapidly cleaves newly secreted ultralarge von Willebrand factor multimers on the endothelial surface under flowing conditions. *Blood.* 2002;100(12):4033-4039.
8. Manz XD, Bogaard HJ, Aman J. Regulation of VWF (Von Willebrand Factor) in Inflammatory Thrombosis. *Arteriosclerosis, Thrombosis, and Vascular Biology.* 2022;42(11):1307-1320.
9. Wendelboe AM, Raskob GE. Global Burden of Thrombosis: Epidemiologic Aspects. *Circ Res.* 2016;118(9):1340-1347.
10. Mackman N, Bergmeier W, Stouffer GA, Weitz JI. Therapeutic strategies for thrombosis: new targets and approaches. *Nature Reviews Drug Discovery.* 2020;19(5):333-352.
11. Spiel AO, Gilbert JC, Jilma B. Von Willebrand Factor in Cardiovascular Disease. *Circulation.* 2008;117(11):1449-1459.
12. El-Mansi S, Nightingale TD. Emerging mechanisms to modulate VWF release from endothelial cells. *The International Journal of Biochemistry & Cell Biology.* 2021;131:105900.
13. Schutgens REG. Aptamers Targeting Von Willebrand Factor: What and Why? *HemaSphere.* 2023;7(2):e830.
14. El-Mansi S, Robinson CL, Kostelnik KB, et al. Proximity proteomics identifies septin and PAK2 as decisive regulators of actomyosin expulsion of von Willebrand factor. *Blood.* 2022.
15. Nightingale TD, White IJ, Doyle EL, et al. Actomyosin II contractility expels von Willebrand factor from Weibel-Palade bodies during exocytosis. *J Cell Biol.* 2011;194(4):613-629.
16. Quintanilla MA, Hammer JA, Beach JR. Non-muscle myosin 2 at a glance. *Journal of Cell Science.* 2023;136(5).
17. McIntosh BB, Ostap EM. Myosin-I molecular motors at a glance. *J Cell Sci.* 2016;129(14):2689-2695.
18. Hartman MA, Spudich JA. The myosin superfamily at a glance. *J Cell Sci.* 2012;125(Pt 7):1627-1632.
19. Woolner S, Bement WM. Unconventional myosins acting unconventionally. *Trends Cell Biol.* 2009;19(6):245-252.
20. Barylko B, Jung G, Albanesi JP. Structure, function, and regulation of myosin 1C. *Acta Biochim Pol.* 2005;52(2):373-380.
21. Zhu T, Beckingham K, Ikebe M. High affinity Ca²⁺ binding sites of calmodulin are critical for the regulation of myosin I beta motor function. *J Biol Chem.* 1998;273(32):20481-20486.
22. Hokanson DE, Laakso JM, Lin T, Sept D, Ostap EM. Myo1c binds phosphoinositides through a putative pleckstrin homology domain. *Mol Biol Cell.* 2006;17(11):4856-4865.
23. Bose A, Guilherme A, Robida SI, et al. Glucose transporter recycling in response to insulin is facilitated by myosin Myo1c. *Nature.* 2002;420(6917):821-824.

24. Cordonnier MN, Dauzon D, Louvard D, Coudrier E. Actin filaments and myosin I alpha cooperate with microtubules for the movement of lysosomes. *Mol Biol Cell*. 2001;12(12):4013-4029.
25. Boguslavsky S, Chiu T, Foley KP, et al. Myo1c binding to submembrane actin mediates insulin-induced tethering of GLUT4 vesicles. *Mol Biol Cell*. 2012;23(20):4065-4078.
26. Kittelberger N, Breunig M, Martin R, Knölker H-J, Miklavc P. The role of myosin 1c and myosin 1b in surfactant exocytosis. *Journal of cell science*. 2016;129(8):1685-1696.
27. Conte IL, Hellen N, Bierings R, et al. Interaction between MyRIP and the actin cytoskeleton regulates Weibel–Palade body trafficking and exocytosis. 2016;129(3):592-603.
28. Nightingale TD, Pattni K, Hume AN, Seabra MC, Cutler DF. Rab27a and MyRIP regulate the amount and multimeric state of VWF released from endothelial cells. *Blood*. 2009;113(20):5010-5018.
29. Li P, Wei G, Cao Y, et al. Myosin IIa is critical for cAMP-mediated endothelial secretion of von Willebrand factor. *Blood*. 2018;131(6):686-698.
30. Holthenrich A, Terplane J, Naß J, Mietkowska M, Kerkhoff E, Gerke V. Spire1 and Myosin Vc promote Ca²⁺-evoked externalization of von Willebrand factor in endothelial cells. *Cellular and Molecular Life Sciences*. 2022;79(2):96.
31. Michaux G, Abbitt KB, Collinson LM, Haberichter SL, Norman KE, Cutler DF. The physiological function of von Willebrand's factor depends on its tubular storage in endothelial Weibel-Palade bodies. *Dev Cell*. 2006;10(2):223-232.
32. Halaszovich CR, Leitner MG, Mavrantoni A, et al. A human phospholipid phosphatase activated by a transmembrane control module. *Journal of Lipid Research*. 2012;53(11):2266-2274.
33. Ruppert C, Godel J, Müller RT, Kroschewski R, Reinhard J, Bähler M. Localization of the rat myosin I molecules myr 1 and myr 2 and in vivo targeting of their tail domains. *J Cell Sci*. 1995;108 (Pt 12):3775-3786.
34. Di Paolo G, Pellegrini L, Letinic K, et al. Recruitment and regulation of phosphatidylinositol phosphate kinase type 1 gamma by the FERM domain of talin. *Nature*. 2002;420(6911):85-89.
35. Romani de Wit T, Rondaij MG, Hordijk PL, Voorberg J, van Mourik JA. Real-time imaging of the dynamics and secretory behavior of Weibel-Palade bodies. *Arterioscler Thromb Vasc Biol*. 2003;23(5):755-761.
36. Riedl J, Crevenna AH, Kessenbrock K, et al. Lifeact: a versatile marker to visualize F-actin. *Nat Methods*. 2008;5(7):605-607.
37. Sun Y, Martin AC, Drubin DG. Endocytic internalization in budding yeast requires coordinated actin nucleation and myosin motor activity. *Dev Cell*. 2006;11(1):33-46.
38. Manenschijn HE, Picco A, Mund M, Rivier-Cordey A-S, Ries J, Kaksonen M. Type-I myosins promote actin polymerization to drive membrane bending in endocytosis. *eLife*. 2019;8:e44215.
39. Edelheit O, Hanukoglu A, Hanukoglu I. Simple and efficient site-directed mutagenesis using two single-primer reactions in parallel to generate mutants for protein structure-function studies. *BMC Biotechnology*. 2009;9(1):61.
40. Owen-Woods C, Joulia R, Barkaway A, et al. Local microvascular leakage promotes trafficking of activated neutrophils to remote organs. *J Clin Invest*. 2020;130(5):2301-2318.
41. Perez-Riverol Y, Bai J, Bandla C, et al. The PRIDE database resources in 2022: a hub for mass spectrometry-based proteomics evidences. *Nucleic Acids Res*. 2022;50(D1):D543-d552.
42. Miklavc P, Frick M. Actin and Myosin in Non-Neuronal Exocytosis. *Cells*. 2020;9(6).
43. Rojo Pulido I, Nightingale TD, Darchen F, Seabra MC, Cutler DF, Gerke V. Myosin Va acts in concert with Rab27a and MyRIP to regulate acute von-Willebrand factor release from endothelial cells. *Traffic*. 2011;12(10):1371-1382.

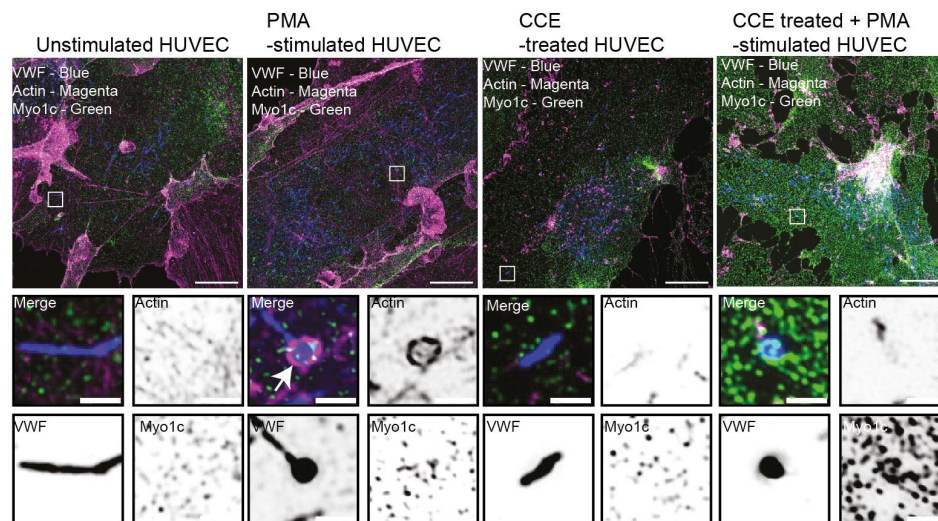
- 622 44. Hanley PJ, Xu Y, Kronlage M, et al. Motorized RhoGAP myosin IXb (Myo9b) controls cell
623 shape and motility. *Proceedings of the National Academy of Sciences*. 2010;107(27):12145-
624 12150.
- 625 45. Rusu L, Andreeva A, Visintine DJ, et al. G protein-dependent basal and evoked endothelial
626 cell vWF secretion. *Blood*. 2014;123(3):442-450.
- 627 46. Mietkowska M, Schuberth C, Wedlich-Soldner R, Gerke V. Actin dynamics during Ca(2+)-
628 dependent exocytosis of endothelial Weibel-Palade bodies. *Biochim Biophys Acta Mol Cell*
629 *Res*. 2019;1866(7):1218-1229.
- 630 47. Brandstaetter H, Kendrick-Jones J, Buss F. Myo1c regulates lipid raft recycling to control cell
631 spreading, migration and Salmonella invasion. *Journal of Cell Science*. 2012;125(8):1991-
632 2003.
- 633 48. Tiwari A, Jung JJ, Inamdar SM, Nihalani D, Choudhury A. The myosin motor Myo1c is
634 required for VEGFR2 delivery to the cell surface and for angiogenic signaling. *Am J Physiol*
635 *Heart Circ Physiol*. 2013;304(5):H687-696.
- 636 49. Bose A, Robida S, Furcinitti PS, et al. Unconventional Myosin Myo1c Promotes Membrane
637 Fusion in a Regulated Exocytic Pathway. *Molecular and Cellular Biology*. 2004;24(12):5447-
638 5458.
- 639 50. Sokac AM, Schietroma C, Gundersen Cameron B, Bement WM. Myosin-1c Couples
640 Assembling Actin to Membranes to Drive Compensatory Endocytosis. *Developmental Cell*.
641 2006;11(5):629-640.
- 642 51. Fan Y, Eswarappa SM, Hitomi M, Fox PL. Myo1c facilitates G-actin transport to the leading
643 edge of migrating endothelial cells. *J Cell Biol*. 2012;198(1):47-55.
- 644 52. Posor Y, Jang W, Haucke V. Phosphoinositides as membrane organizers. *Nature Reviews*
645 *Molecular Cell Biology*. 2022;23(12):797-816.
- 646 53. Ammar M, Kassas N, Chasserot-Golaz S, Bader M-F, Vitale N. Lipids in Regulated Exocytosis:
647 What are They Doing? *Frontiers in Endocrinology*. 2013;4.
- 648 54. Disse J, Vitale N, Bader MF, Gerke V. Phospholipase D1 is specifically required for regulated
649 secretion of von Willebrand factor from endothelial cells. *Blood*. 2009;113(4):973-980.
- 650 55. Nguyen TTN, Koerdt SN, Gerke V. Plasma membrane phosphatidylinositol (4,5)-bisphosphate
651 promotes Weibel-Palade body exocytosis. *Life Sci Alliance*. 2020;3(11).
- 652 56. Chinthalapudi K, Taft MH, Martin R, et al. Mechanism and specificity of
653 pentachloropseudilin-mediated inhibition of myosin motor activity. *J Biol Chem*.
654 2011;286(34):29700-29708.
- 655 57. Nightingale TD, McCormack JJ, Grimes W, et al. Tuning the endothelial response: differential
656 release of exocytic cargos from Weibel-Palade bodies. *J Thromb Haemost*. 2018;16(9):1873-
657 1886.
- 658 58. Holthenrich A, Terglane J, Naß J, Mietkowska M, Kerkhoff E, Gerke V. Spire1 and Myosin Vc
659 promote Ca(2+)-evoked externalization of von Willebrand factor in endothelial cells. *Cell Mol*
660 *Life Sci*. 2022;79(2):96.
- 661 59. Han X, Li P, Yang Z, et al. Zyxin regulates endothelial von Willebrand factor secretion by
662 reorganizing actin filaments around exocytic granules. *Nature Communications*.
663 2017;8(1):14639.
- 664 60. Schietroma C, Yu HY, Wagner MC, Umbach JA, Bement WM, Gundersen CB. A role for
665 myosin 1e in cortical granule exocytosis in *Xenopus* oocytes. *J Biol Chem*.
666 2007;282(40):29504-29513.
- 667 61. Toyoda T, An D, Witczak CA, et al. Myo1c Regulates Glucose Uptake in Mouse Skeletal
668 Muscle ^{*}. *Journal of Biological Chemistry*. 2011;286(6):4133-4140.
- 669 62. Capmany A, Yoshimura A, Kerdous R, et al. MYO1C stabilizes actin and facilitates the arrival
670 of transport carriers at the Golgi complex. *J Cell Sci*. 2019;132(8).

63. Brandstaetter H, Kishi-Itakura C, Tumbarello DA, Manstein DJ, Buss F. Loss of functional MYO1C/myosin 1c, a motor protein involved in lipid raft trafficking, disrupts autophagosome-lysosome fusion. *Autophagy*. 2014;10(12):2310-2323.
64. Almeida CG, Yamada A, Tenza D, Louvard D, Raposo G, Coudrier E. Myosin 1b promotes the formation of post-Golgi carriers by regulating actin assembly and membrane remodelling at the trans-Golgi network. *Nat Cell Biol*. 2011;13(7):779-789.
65. Tokuo H, Komaba S, Coluccio LM. In pancreatic β -cells myosin 1b regulates glucose-stimulated insulin secretion by modulating an early step in insulin granule trafficking from the Golgi. *Mol Biol Cell*. 2021;32(12):1210-1220.
66. Delestre-Delacour C, Carmon O, Laguerre F, et al. Myosin 1b and F-actin are involved in the control of secretory granule biogenesis. *Scientific Reports*. 2017;7(1):5172.
67. Yu HY, Bement WM. Multiple myosins are required to coordinate actin assembly with coat compression during compensatory endocytosis. *Mol Biol Cell*. 2007;18(10):4096-4105.
68. Miklavc P, Ehinger K, Sultan A, et al. Actin depolymerisation and crosslinking join forces with myosin II to contract actin coats on fused secretory vesicles. *Journal of Cell Science*. 2015;128(6):1193-1203.
69. Milberg O, Shitara A, Ebrahim S, et al. Concerted actions of distinct nonmuscle myosin II isoforms drive intracellular membrane remodeling in live animals. *J Cell Biol*. 2017;216(7):1925-1936.
70. Tran DT, Masedunskas A, Weigert R, Ten Hagen KG. Arp2/3-mediated F-actin formation controls regulated exocytosis in vivo. *Nature Communications*. 2015;6(1):10098.

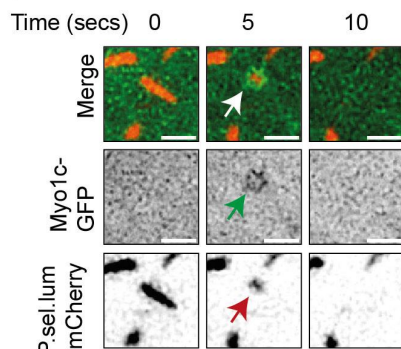
Figure 1



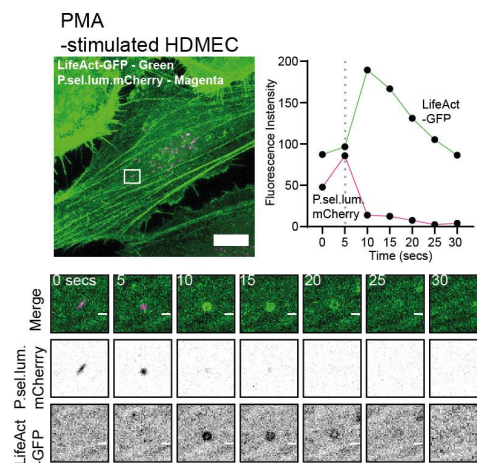
A



B



C



D

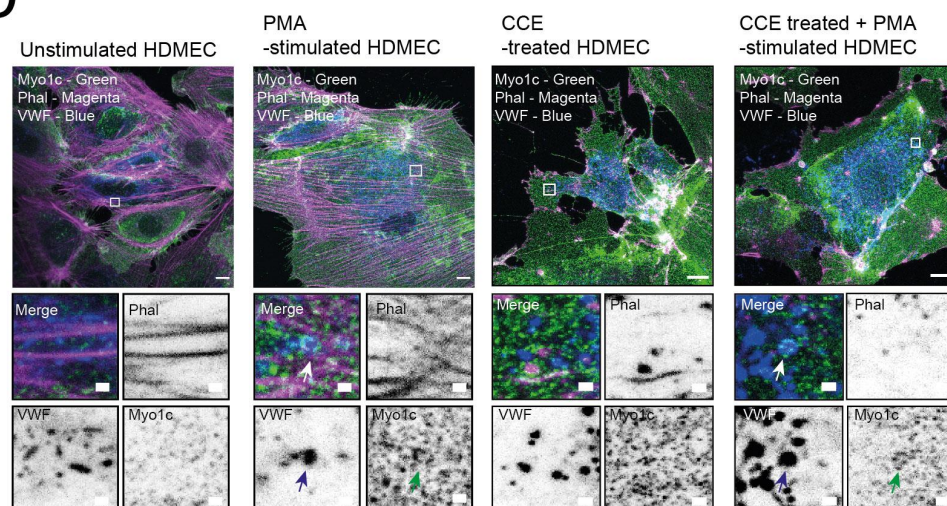


Figure 3

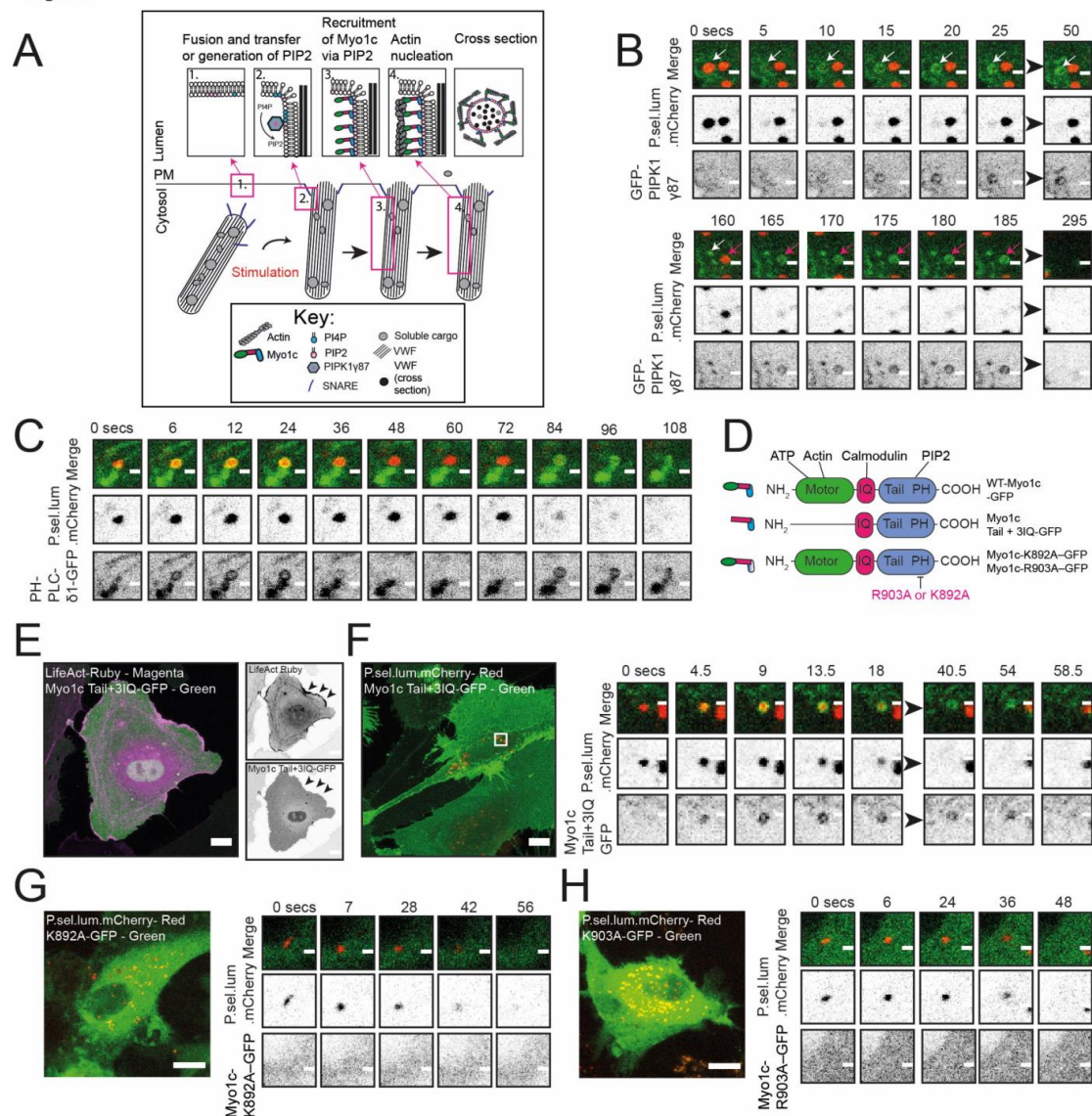


Figure 4

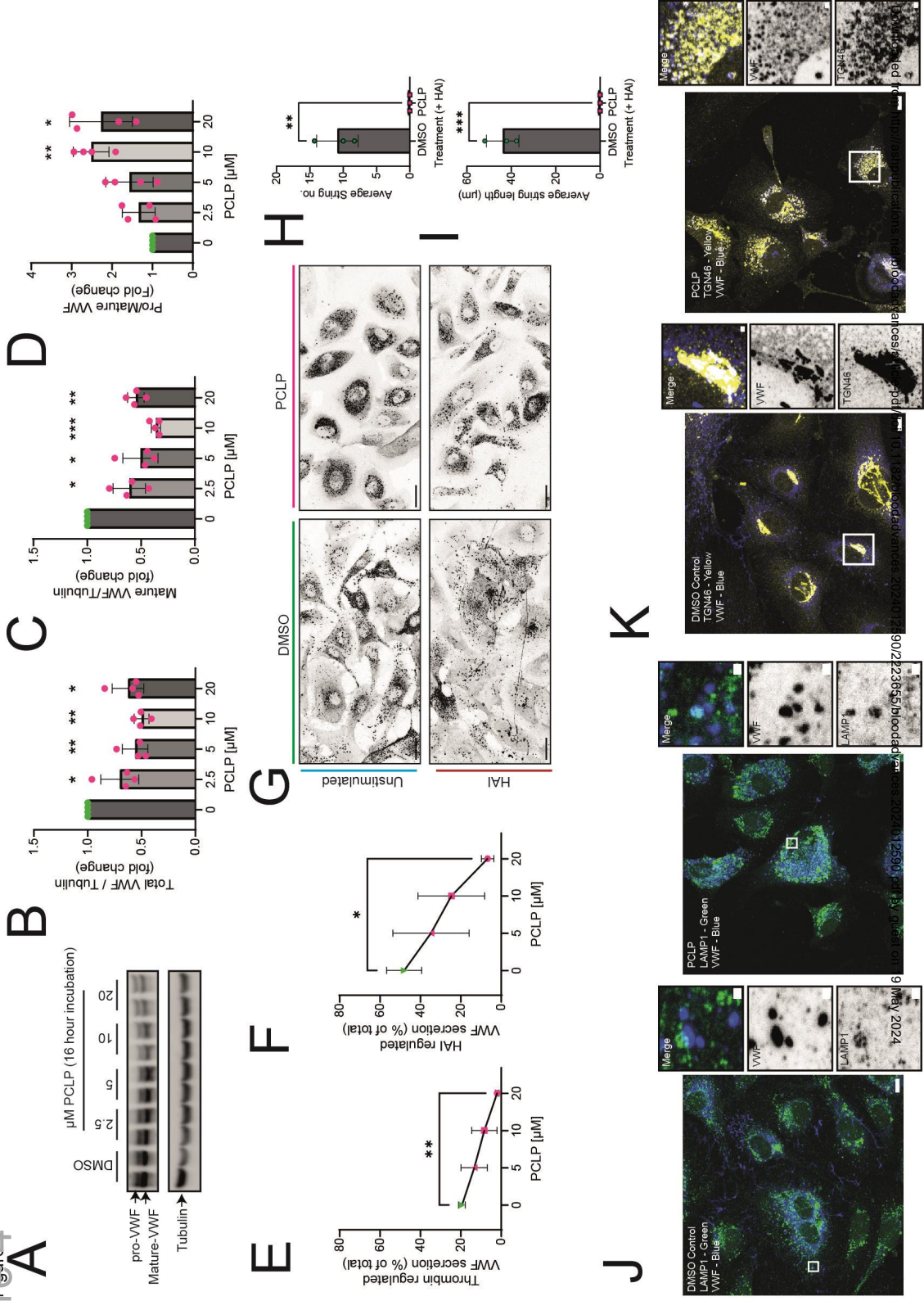


Figure 5

Figure 5

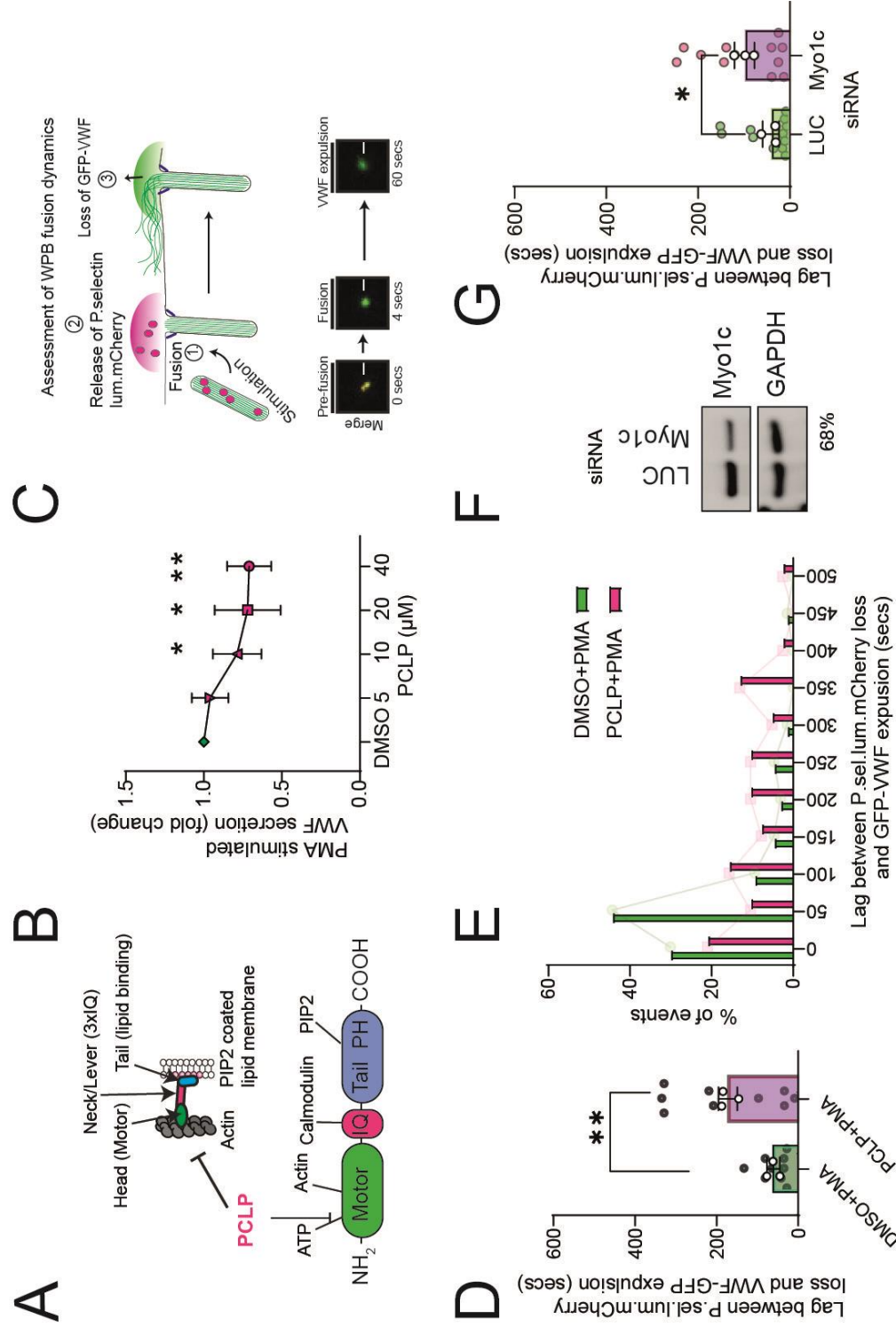


Figure 6

